

Electron scattering from hexafluoroacetone molecules: cross section measurements and calculations

This article has been downloaded from IOPscience. Please scroll down to see the full text article.

2011 J. Phys. B: At. Mol. Opt. Phys. 44 205202

(<http://iopscience.iop.org/0953-4075/44/20/205202>)

View [the table of contents for this issue](#), or go to the [journal homepage](#) for more

Download details:

IP Address: 153.19.58.31

The article was downloaded on 25/10/2011 at 18:04

Please note that [terms and conditions apply](#).

Electron scattering from hexafluoroacetone molecules: cross section measurements and calculations

Czesław Szmytkowski, Paweł Możejko and Elżbieta Ptańska-Denga

Atomic Physics Division, Department of Atomic Physics and Luminescence, Faculty of Applied Physics and Mathematics, Gdańsk University of Technology, ul. Gabriela Narutowicza 11/12, 80-233 Gdańsk, Poland

E-mail: czsz@mif.pg.gda.pl and paw@mif.pg.gda.pl

Received 5 July 2011, in final form 19 August 2011

Published 23 September 2011

Online at stacks.iop.org/JPhysB/44/205202

Abstract

Absolute total cross section (TCS) for electron scattering from hexafluoroacetone (HFA: $(\text{CF}_3)_2\text{CO}$) molecules has been measured from 1 to 400 eV, employing a linear electron-transmission technique. The TCS energy function for the electron–HFA collision has two broad enhancements: the first, visible between 2 and 28 eV, can be partly attributed to resonant processes; the second is much broader, centred around 50 eV, and is characteristic of perfluorinated targets. The low-energy enhancement is superimposed with weak features perceptible near 3.6, 8.5 and 17 eV. Calculations were carried out for HFA and for acetone to obtain the integral elastic and ionization cross sections at intermediate and high incident energies, using the independent atom approximation and binary-encounter-Bethe approach, respectively. The computed total (elastic plus ionization) cross sections are above 70 eV in reasonable agreement with the experimental TCSs. A comparison is made between cross sections for HFA and its per-hydrogenated counterpart, acetone ($(\text{CH}_3)_2\text{CO}$); the effect of perfluorination is indicated.

(Some figures in this article are in colour only in the electronic version)

1. Introduction

The basic ideas and the fundamental quantities concerning the electron interaction with components of matter (atoms, molecules and clusters) are indispensable for understanding, modelling and controlling processes in which electrons are involved. Applications of electron-collision data range from purely scientific (e.g. atomic physics, physico-chemistry of interstellar and environmental media) to industrial (plasma-based processing, energy conversion) uses. The recent discovery that slow electrons can induce strand breaks in the DNA (Boudaïffa *et al* 2000) has renewed interest in electron interaction with molecules of biological importance. Despite a growing demand for electron-assisted data (cross sections, transport coefficients, reaction rates) and a great effort to gain them in extensive studies, the availability of comprehensive and reliable sets of quantitative electron-impact data—especially those in absolute scale—is still far from satisfactory.

For a hexafluoroacetone (HFA: $(\text{CF}_3)_2\text{CO}$) molecule, a fluorine-substituted counterpart of acetone ($(\text{CH}_3)_2\text{CO}$), investigations of electron-impact processes have received only moderate interest so far. Experimental studies of electron–HFA collision phenomena have been primarily focused on the formation of negative and positive ions. Investigations of the electron attachment to the HFA molecule leading to the generation of negative ions at low impact energies were carried out first by Thynne (1968), Harland and Thynne (1969, 1970), Naff *et al* (1972) and more recently by Martin (2007) and Martin *et al* (2009). The formation of positive ions in direct ionization and via dissociative channels has been studied by Harland and Thynne (1970). In these experiments, the intensities of the negative and positive ion mass spectra were obtained in arbitrary units only. Hilderbrandt *et al* (1970) determined the HFA molecular geometry by the gas-phase electron diffraction. To our knowledge, there are no reports in the literature on measurements and computations of the

Table 1. Absolute electron-scattering TCSs for hexafluoroacetone, (CF₃)₂CO, molecules, in units of 10⁻²⁰ m².

E (eV)	TCS	E (eV)	TCS	E (eV)	TCS	E (eV)	TCS	E (eV)	TCS
1	28.6	3.6	30.9	7.0	40.5	19	40.2	90	39.1
1.2	28.0	3.8	31.1	7.5	40.6	21	39.6	100	37.6
1.4	27.6	4.0	31.8	8.0	40.7	22.5	38.9	110	36.5
1.6	27.4	4.2	32.6	8.5	40.8	26	38.5	120	35.4
1.8	27.2	4.4	33.6	9.0	40.6	27.5	38.3	140	33.4
2.0	27.2	4.6	34.4	9.5	40.5	30	38.7	160	31.3
2.2	27.4	4.8	35.6	10.0	40.4	35	41.1	180	29.2
2.4	27.5	5.0	36.7	10.5	40.4	40	42.7	200	27.5
2.6	27.8	5.2	37.9	11	40.2	45	43.4	220	26.0
2.8	28.1	5.5	38.8	12	40.2	50	43.6	250	24.1
3.0	28.5	5.7	39.3	13	40.2	60	43.0	300	21.5
3.2	29.4	6.0	39.8	15	40.3	70	41.7	350	19.3
3.4	30.3	6.5	40.2	17	40.3	80	40.3	400	17.6

total electron-scattering cross section for HFA. Such a limited number of works for HFA is in contrast to its per-hydrogenated analogue, acetone, for which extensive studies on the electron impact have been performed (see, e.g., Szmytkowski (2010)).

The main goal of this work is to provide absolute values of *grand* total cross sections (TCSs) for the electron–HFA scattering over wide impact energy range, from low (1 eV) to intermediates (400 eV). For energies above the present experimental energy range, the measured TCS results are complemented with the sum (ECS + ICS) of integral elastic cross section (ECS) and ionization cross section (ICS) calculated in this work. To find how the replacement of fluorine atoms with hydrogen reflects in the electron-scattering cross sections, the results for HFA are then compared with the data for acetone.

2. Experimental procedure

The absolute electron-scattering TCS measurements presented in this work have been carried out on our electron spectrometer working in the linear transmission mode. The electrons are provided by an electron gun coupled to an electrostatic 127° cylindrical monochromator and followed with an electron lens system. The electron beam of given energy E and an energy resolution of $\Delta E \simeq 0.1$ eV (FWHM) is directed into a gas-target cell of 30.5 mm length. The electrons emerging from the reaction volume through the exit aperture meet a retarding potential analyser (RPA). The RPA unit reduces the number of inelastically scattered electrons which might be accepted by the Faraday cup (FC) collector. The acceptance angle of the detector system, defined by the electron lens apertures, is 0.8 msr. The intensities, $I(E)$, of the transmitted electrons collected by the FC are measured with a Keithley 617 electrometer. Other quantities taken in the experiment necessary for the TCS, $Q(E)$, determination are the target vapour pressure in the scattering chamber, p , and its temperature, T_t .

The TCS is derived based on the Bouguer–de Beer–Lambert (BBL) attenuation formula

$$I(E, p) = I(E, 0) \exp \left[-\frac{Q(E)pL}{k\sqrt{T_t T_m}} \right],$$

where $I(E, p)$ and $I(E, 0)$ are the intensities of the electron beam currents transmitted through the scattering cell, taken in the presence and absence of the target, respectively. When the vapour under study is let into the reaction cell, its pressure, p , is maintained at the level of 0.05–0.2 Pa that prevents multiple-scattering events. As the temperature of the absolute manometer head, $T_m = 322$ K, is a few degrees higher than that of the target vapour in the scattering cell, T_t , the thermal transpiration formula (Knudsen 1910) is applied to convert the pressure reading into the target pressure, p . L represents the effective length of the electron pathway within the target, approximated with the distance between entrance and exit cell apertures. k is the Boltzmann constant. The target vapour pressure in the scattering chamber is measured using MKS Baratron capacitance gauge with a stated accuracy of 0.5%. The intensity of the ambient magnetic field along the electron pathway in the electron optics region is kept below 0.1 μ T. This ensures that the trajectories of the unscattered electrons are straight lines within the scattering and the detector volumes. The spectrometer electron optics is housed in a vacuum chamber with the background pressure lower than 40 μ Pa. The uncertainty of the energy scale is about 0.15 eV, mostly due to the shift in the contact potentials, related to the target molecules deposition on the electron optics elements in the course of the long-lasting experiment. Energy setting, handling the gas target, collection and processing ingoing data were operated under computer control. Other details of the experimental arrangement and data processing employed have been described elsewhere (Szmytkowski *et al* 1997, Szmytkowski and Mozejko 2001).

The quantities used for the TCS derivation are taken directly in the present experiment, so the TCSs for HFA, listed in table 1 and shown in figure 2, are in absolute scale. The statistical uncertainty (one standard deviation of the weighted mean value) of the measured TCS does not exceed 1% over the entire energy range investigated. An accuracy of the measured TCS suffers significantly from the effects which systematically disturb the foundations of the BBL attenuation relationship employed in the electron-transmission method (Bederson and Kieffer 1971). The most troublesome uncertainty of the measured TCS is related to a finite angular discrimination of electrons which leave the scattering volume through the

exit orifice: the detector system does not distinguish electrons scattered elastically into small forward angles from those not scattered (transmitted only). Therefore, the measured intensity of transmitted electrons, $I(E, p)$, is usually overestimated leading to systematic lowering of the measured TCS from its exact value. The effect is particularly meaningful for targets of large permanent electric dipole moment and/or of large dipole polarizability, and is, at least in part, the reason of distinct discrepancies (even by the factor of 2) among TCSs measured in different laboratories as well as between experiments and contemporary calculations (Khakoo *et al* 2009). Very recently, Sullivan *et al* (2011) have demonstrated that even small changes in the degree of forward-angle discrimination can lead to significant changes both in the magnitude and shape of the measured TCSs. The way to reduce the TCS underestimation for the target under study is, first, to improve the forward-angle discrimination and, second, to estimate the effect of the forwardly scattered electrons and to correct the measured data. For the correction, however, the absolute differential cross sections (DCSs) from experiments and/or calculations and the detector discrimination angle at each given electron energy are necessary. Unfortunately, the angular distribution data for the HFA molecule are currently not available in the literature. Therefore, for the estimation of the potential TCS lowering due to forward-angle scattering, we used at intermediate energies (100–400 eV), the elastic DCSs calculated in this work, while at low impact energies the calculations of Bettega and Lima (2007) for the furan molecule which has low electric dipole moment and the geometric size similar to that of HFA. We found that the inability to discriminate against electrons which are scattered elastically through the small angles in the forward direction may systematically lower the measured TCS by about 6–8% at the lowest and by 3–5% at intermediate impact energies used. As these estimations, especially at low energies, are rather crude; the TCS data reported in this work (listed in table 1) are not corrected for the forward-angle scattering effect.

The HFA sample of a stated purity 97%, from Sigma-Aldrich, was used directly from a supplied cylinder without any further purification. Before starting the TCS measurements, the electron optics was passivated in the presence of the HFA for some hours, until the filament emission and the electron transmission became stabilized. After this procedure was applied, the TCS values obtained at the same energy were, within the random experimental uncertainties, independent of the applied target pressures and the electron-beam intensities (0.04–20 pA). We found that after opening/closing the gas valve, a delay of about 1 min was sufficient to stabilize the target conditions in the scattering cell. To keep the conditions in the electron optics volume invariable throughout the experiment, irrespective of whether the target is present or absent in the scattering cell, the target vapour was supplied alternately into the collision cell or its surrounding, so the residual target pressure in the electron optics region is below 0.1 mPa and practically constant in the course of the experiment. The inevitable effusion of the target particles through orifices of the scattering cell also leads to inhomogeneity of the target density in the reaction

volume and to elongation of the effective path over which the scattering events may take place. Calculations show that for the geometry of the reaction cell applied in our experiment, the error related to the factor pL in the BBL formula is less than 2% (Nelson and Colgate 1973). Finally, the question arises: what is the TCS uncertainty related to impurities present in the sample used? The presence of residual impurities which have a strong permanent electric dipole moment might increase the measured TCS quite markedly, especially at the lowest electron impact energies. However, the behaviour of the low-energy TCS obtained for HFA (figure 2) suggests that highly polar impurities are rather insignificant in our experiment. As details on the impurities present in the HFA sample are not available, we have assumed the uncertainty of the measured TCS resulting from the uncertainty of the target purity to be equal of 3%. Other possible TCS systematic error components are estimated to be less than 1% each. The overall systematic uncertainty of our measured absolute TCS, evaluated as a sum of possible systematic errors, amounts to 14–16% below 3 eV, 6–10% within 5–150 eV and 7–9% at higher energies applied.

3. Cross section calculations

To extend the range of energy beyond that for which the e^- -HFA TCS has been measured in the present experiment (1–400 eV), computations of the ECS and ICS have been carried out at intermediate and high impact energies. The sum of both calculated partial cross sections represents the computational TCS. The approximation of the TCS with the sum of only elastic and ionization components is validated because ionization typically predominates over other inelastic contributions at intermediate and high collision energies. Our previous investigations have supported the expectation that TCS obtained with this approach satisfactorily reproduces the intermediate-energy experimental data for a variety of simple and complex molecular targets (Domaracka *et al* 2006, 2007, Szmytkowski and Mozejko 2006, Szmytkowski *et al* 2007, 2010). Cross sections for the elastic scattering have been obtained applying the independent atom method (IAM) (Mott and Massey 1965, Raj 1991). Electron-impact ionization cross sections have been calculated using the binary-encounter-Bethe (BEB) formalism (Kim and Rudd 1994, Hwang *et al* 1996). To have in hand respective data for comparison, computations have also been done for acetone molecule, the hydrogen-substituted analogue of HFA. Since both theoretical methods and computational procedures used in the present calculations have been described in our previous work (e.g. Mozejko *et al* 2002, Mozejko and Sanche 2003, 2005, Szmytkowski *et al* 2007), only a brief overview is provided here.

Within the IAM approach, the electron–molecule elastic collision is reduced to a more simple problem of the electron elastic scattering from individual atoms constituting the target molecule, assuming that electrons possess sufficiently high energies. Then, the DCS for elastic electron-scattering on

molecule, taking into account all possible orientations of the intermolecular axis, is given as

$$\frac{d\sigma}{d\Omega} = \sum_i^N \sum_j^N f_i(\theta, k) f_j^*(\theta, k) \frac{\sin(sr_{ij})}{sr_{ij}}, \quad (1)$$

where N is the number of atoms within the molecule, θ is the scattering angle and $f_i(\theta, k)$ and $f_j(\theta, k)$ are complex scattering amplitudes due to the i th and j th atom of the molecule, respectively. $s = 2k \sin(\theta/2)$ is the magnitude of the momentum transfer during the collision and k is the wave number of the incident electron. The distance between the i th and j th atom is denoted as r_{ij} .

The integral ECS for the electron–molecule scattering in this approximation is given by

$$\sigma(E) = \sum_{i=1}^N \sigma_i(E), \quad (2)$$

where $\sigma_i(E)$ is the ECS for scattering on the i th atom of the molecule, and $E = k^2/2$ is the energy of the incident electron.

To obtain atomic scattering amplitudes and the elastic electron–atom cross sections, we employed a partial wave analysis and numerically solved the radial Schrödinger equation

$$\left[\frac{d^2}{dr^2} - \frac{l(l+1)}{r^2} + k^2 - 2(V_{\text{stat}}(r) + V_{\text{polar}}(r)) \right] u_l(r) = 0 \quad (3)$$

under the boundary conditions

$$u_l(0) = 0, \quad u_l(r) \xrightarrow{r \rightarrow \infty} A_l \hat{j}_l(kr) - B_l \hat{n}_l(kr), \quad (4)$$

where $\hat{j}_l(kr)$ and $\hat{n}_l(kr)$ are the spherical Bessel–Riccati and Neumann–Riccati functions, respectively. $V_{\text{stat}}(r)$ is the static potential of the atom determined following the procedure of Salvat *et al* (1987):

$$V_{\text{stat}}(r) = -\frac{Z}{r} \sum_{i=1}^3 a_i \exp(-\beta_i r), \quad (5)$$

where Z is the nuclear charge of the i th atom, and β_i and a_i are the parameters determined by an analytical fitting procedure to Dirac–Hartree–Fock–Slater self-consistent data. The polarization potential $V_{\text{polar}}(r)$ was expressed in the form proposed by Padial and Norcross (1984)

$$V_{\text{polar}}(r) = \begin{cases} v(r) & r \leq r_c \\ -\alpha/2r^4 & r > r_c \end{cases}, \quad (6)$$

where $v(r)$ is the free-electron–gas correlation energy (Pedrew and Zunger 1981), α is the static electric dipole polarizability of the atom, while r_c is the first crossing point of the $v(r)$ and $-\alpha/2r^4$ curves (Zhang *et al* 1992).

The scattering amplitudes for the electron–atom scattering were obtained using the following equation:

$$f(\theta, k) = \frac{1}{2ik} \sum_{l=0}^{l_{\text{max}}} (2l+1) (e^{2i\delta_l} - 1) P_l(\cos \theta) + \pi \alpha k \left(\frac{1}{3} - \frac{1}{2} \sin \frac{\theta}{2} - \sum_{l=1}^{l_{\text{max}}} \frac{P_l(\cos \theta)}{(2l-1)(2l+3)} \right), \quad (7)$$

where $P_l(\cos \theta)$ are Legendre polynomials, $l_{\text{max}} = 100$ and the second term in the above equation is the Born scattering amplitude for the potential of the form proposed by Mott and Massey (1965).

The integral cross sections for elastic electron–atom scattering were derived from the expression

$$\sigma = \frac{4\pi}{k^2} \left(\sum_{l=0}^{l_{\text{max}}} (2l+1) \sin^2 \delta_l + \sum_{l=l_{\text{max}+1}}^{\infty} (2l+1) \sin^2 \delta_l^{(B)} \right), \quad (8)$$

where δ_l^B represents the phase shift evaluated in the Born approximation. DCSs for elastic electron scattering from atoms were calculated employing a normalization procedure (Maljković *et al* 2009), according to

$$\frac{d\sigma}{d\Omega} = |f(\theta, k)|^2. \quad (9)$$

Within the BEB model, the cross section for electron–impact ionization, σ^{Ion} , can be obtained as

$$\sigma^{\text{Ion}} = \sum_{i=1}^{n_{\text{MO}}} \sigma_i^{\text{BEB}}, \quad (10)$$

where n_{MO} is the number of the given molecular orbital. The electron–impact ionization cross section per molecular orbital is given by the following expression:

$$\sigma^{\text{BEB}} = \frac{S}{t+u+1} \left[\frac{\ln t}{2} \left(1 - \frac{1}{t^2} \right) + 1 - \frac{1}{t} - \frac{\ln t}{t+1} \right], \quad (11)$$

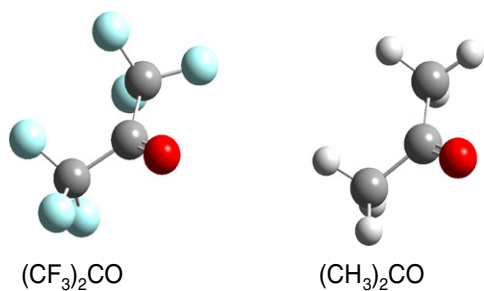
where $u = U/B$, $t = T/B$, $S = 4\pi a_0^2 N R^2 / B^2$, $a_0 = 0.5292 \text{ \AA}$, $R = 13.61 \text{ eV}$ and T is the energy of the impinging electron. The electron binding energy, B , kinetic energy of the orbital, U , and orbital occupation number, N , have been calculated for the ground states of the geometrically optimized, within the C_2 symmetry, molecules (cf figure 1). For calculations, the Hartree–Fock method using the GAUSSIAN code of Frisch *et al* (2003), and built in the standard Gaussian 6-31G+ basis set, has been employed. For that molecular geometry, the obtained dipole moment of HFA ($\mu = 0.56 \text{ D}$) appears to be smaller than for acetone molecules ($\mu = 3.38 \text{ D}$), in accordance with experiments (see table 3). Because energies of the highest occupied molecular orbitals (HOMO) obtained in this way usually differ from experimental ones, we also performed the outer valence Green function calculations of correlated electron affinities and ionization potentials (Cederbaum 1975, von Niessen *et al* 1984, Ortiz 1988, Zakrzewski and von Niessen 1994) using the GAUSSIAN code (Frisch *et al* 2003).

4. Results and discussion

Using the linear-transmission technique, we measured absolute electron-scattering TCSs for the hexafluoroacetone ((CF₃)₂CO: HFA) molecule. The present TCS results are shown graphically in figure 2 and the numerical experimental TCS values from 1 to 400 eV are listed in table 1. Comparison of the measured TCS energy dependence for (CF₃)₂CO with earlier experimental TCS data for acetone ((CH₃)₂CO) is made in figure 3 and the perfluorination effect is indicated. The integral ECS and ICS have been calculated for HFA and

Table 2. ICS and integral ECS calculated for electron impact on $(\text{CF}_3)_2\text{CO}$ (HFA) and $(\text{CH}_3)_2\text{CO}$ (A) molecules, in 10^{-20} m^2 .

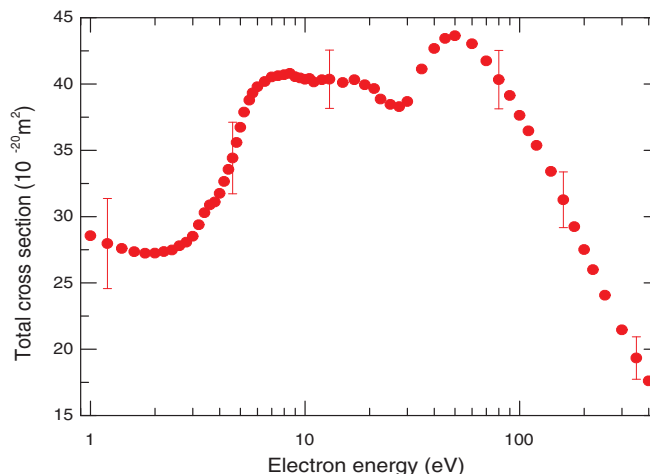
E (eV)	ICS		ECS		E (eV)	ICS		ECS	
	HFA	A	HFA	A		HFA	A	HFA	A
9.793		0			110	11.42	9.12	23.7	13.8
10		0.0185			120	11.45	8.95	22.4	13.0
11		0.114			140	11.36	8.59	20.3	11.7
11.915	0				160	11.16	8.22	18.7	10.6
12	0.0415	0.212			180	10.91	7.86	17.4	9.78
13	0.0557	0.317			200	10.63	7.52	16.3	9.08
14	0.110	0.499			220			15.3	8.49
15	0.164	0.803			225	10.27	7.13		
16	0.221	1.13			250	9.91	6.76	14.2	7.75
17	0.366	1.56			300	9.23	6.14	12.6	6.79
18	0.600	1.99			350	8.61	5.62	11.4	6.06
19	0.898	2.41			400	8.06	5.18	10.5	5.48
20	1.22	2.82			450	7.57	4.81	9.68	5.01
22.5	2.00	3.77			500	7.14	4.49	9.01	4.62
25	2.80	4.58			600	6.41	3.97	7.94	4.00
27.5	3.62	5.28			700	5.82	3.56	7.11	3.53
30	4.38	5.91	66.9	38.0	800	5.33	3.23	6.45	3.17
35	5.73	6.92	57.8	33.2	900	4.92	2.96	5.91	2.87
40	6.82	7.67	51.2	29.6	1000	4.58	2.74	5.45	2.63
45	7.71	8.23	46.1	26.9	1100			5.07	2.43
50	8.45	8.63	42.1	24.7	1200			4.74	2.26
55	9.08	8.92			1400			4.21	1.99
60	9.59	9.13	36.4	21.4	1500	3.41	2.00		
65	10.01	9.26			1600			3.79	1.79
70	10.34	9.35	32.3	19.1	1800			3.46	1.63
75	10.62	9.39			2000	2.74	1.59	3.20	1.51
80	10.84	9.41	29.4	17.3	2200			2.99	1.42
85	11.01	9.40			2500	2.29	1.32	2.74	1.32
90	11.15	9.36	27.0	15.9	3000	1.98	1.14	2.48	1.25
95	11.25	9.32			3500	1.75	1.00		
100	11.33	9.26	25.2	14.8	4000	1.566	0.895		

**Figure 1.** Schematic of the HFA ($(\text{CF}_3)_2\text{CO}$) geometry. For comparison, the geometry of acetone ($(\text{CH}_3)_2\text{CO}$) molecule is shown.

acetone molecules at intermediate and high incident energies using the IAM and the BEB approach, respectively; results are presented in table 2. The computed TCSs (ECS + ICS) for HFA and acetone are confronted with the experimental findings in figure 3.

4.1. Electron-scattering cross sections for hexafluoroacetone: $(\text{CF}_3)_2\text{CO}$

Figure 2 shows the energy dependence of our absolute TCS for the electron–HFA scattering measured from 1 to 400 eV. The following discussion of the experimental TCS energy

**Figure 2.** Experimental, absolute total electron-scattering cross section (TCS) for hexafluoroacetone, $(\text{CF}_3)_2\text{CO}$, molecule: (\bullet), present; error bars represent overall uncertainties.

behaviour has a rather qualitative character as it is mainly based on electron-scattering data available in arbitrary units only.

Regarding the variability of the present experimental TCS energy function, three regions can be distinguished, delimited with two minima. In the lowest (1–2 eV) energy region

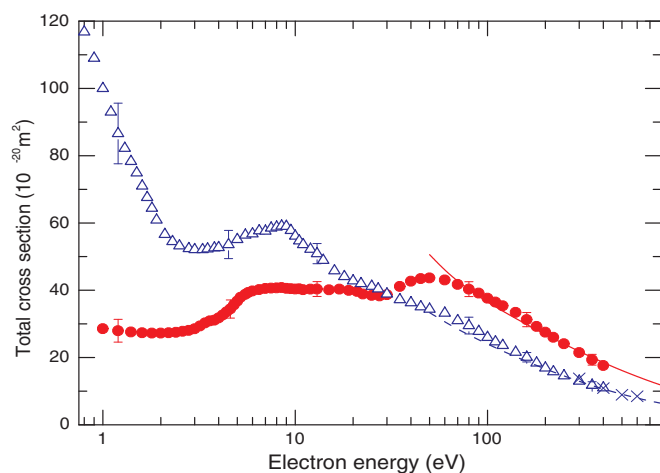


Figure 3. Illustration of the perfluorination effect. The present experimental TCS for electron scattering from hexafluoroacetone, $(\text{CF}_3)_2\text{CO}$, (\bullet) is compared with the TCSs measured for the acetone, $(\text{CH}_3)_2\text{CO}$, molecule: (Δ), absolute (Szmytkowski 2010), overall errors are indicated; (\times), (Kimura *et al* 2000), normalized, for the sake of legibility only results above 300 eV are included. Displayed are intermediate-energy total (elastic plus ionization) cross sections also calculated in this work: HFA (—); acetone (- - -).

studied, the TCS decreases slowly from $28.5 \times 10^{-20} \text{ m}^2$ at 1 eV to about $27.2 \times 10^{-20} \text{ m}^2$ in the vicinity of 1.9 eV where the first minimum is located. Although we could not measure the TCS below 1 eV in the present experiment, it is worth making some remarks anticipating the TCS behaviour at thermal energies. There are arguments, related both to direct and resonant electron–HFA scattering channels, for the steep increase of the TCS towards zero energy. The resonant scattering appears when the impinging electron of proper energy is temporarily attached to the target molecule forming a short-lived negative ion state (resonance). The transient negative ion can subsequently decompose either via a dissociative channel involving the formation of negative and neutral fragments, and/or through a competitive autodetachment channel which leaves the parent molecule in one of the vibrational states. Experiments (Thynne 1968, Harland and Thynne 1969, 1970, Naff *et al* 1972, Martin 2007, Martin *et al* 2009) show that the HFA molecule effectively captures thermal electrons into a temporary parent negative ion state, $(\text{CF}_3)_2\text{CO}^-$, with an autodetachment lifetime of about 65 μs (Naff *et al* 1972). Harland and Thynne (1969, 1970) determined the ratio of cross sections for the electron attachment to SF_6 and HFA molecules; $\sigma_{\text{SF}_6}/\sigma_{\text{HFA}} = 58.9$ has been reported close to 0 eV. Combining this value with the electron attachment cross section for SF_6 , $\sigma_{\text{SF}_6} = 7.6 \times 10^{-17} \text{ m}^2$ at 0.0001 eV (recommended recently by Christophorou and Olthoff 2004), one obtains $\sigma_{\text{HFA}} \approx 1.3 \times 10^{-18} \text{ m}^2$ near zero energy, a value more than four times higher than the present TCS taken at 1 eV. Near zero electron volts, Martin (2007) also noticed a weak signal of C_3F_4^- fragment ions, formed in the dissociative electron-attachment scattering channel. Another argument for the increase of TCS below 1 eV comes from the fact that the HFA molecule has permanent, although moderate, electric dipole moment (see table 3) and that for polar molecules the electron-scattering cross section increases towards zero energy. Such

Table 3. Electrical parameters of $(\text{CH}_3)_2\text{CO}$ and $(\text{CF}_3)_2\text{CO}$ compounds: permanent electric dipole moment (μ); electrical polarizability (α).

Molecule	μ (Debye)	α (10^{-30} m^3)
$(\text{CH}_3)_2\text{CO}$	2.88 ^a	9.7 ^a
$(\text{CF}_3)_2\text{CO}$	0.39 ^b ; 0.56 ^c ; 0.65 ^d	7.5 ^e ; 7.8 ^f

^a From Lide (1995–1996).

^b Experiment of Grabow *et al* (1991).

^c Present calculations.

^d Experiment of Chan (1969).

^e Estimated by Mazurek *et al* (2002), employing the data for acetone and fluorinated methanes $\text{CH}_n\text{F}_{4-n}$.

^f Present estimation based on the additivity formula (Miller 1990).

behaviour of the low-energy TCS is explained in terms of the direct scattering in which the long-range interaction of the impinging electron with polar target dominates (Itikawa 1978).

Above 2 eV, the measured TCS energy function exhibits prominent enhancement; between 3 and 6 eV the TCS increases by more than 30%. Previous experiments on the e^- –HFA scattering show that some contribution to this enhancement comes from resonant scattering phenomena. Within 2 and 9 eV, numerous fragment anions have been observed by Thynne (1968), Harland and Thynne (1969, 1970), Naff *et al* (1972), Martin (2007) and Martin *et al* (2009), although much less abundant than the parent anion formed at ~ 0 eV. In the vicinity of 3.2 eV, the formation of F^- , CF_3^- , CF_3CO^- and $\text{CF}_3\text{COCF}_2^-$ was evidenced, while around 6 eV, only F^- and CF_3^- ions were detected (Martin 2007). A change in the slope of the TCS curve visible between 3 and 4 eV can be attributed to the structures observed in the electron attachment spectra near 3.2 eV. Unfortunately, yields of these anions have been reported in relative units, which does not allow us to estimate the proportion in which particular resonant channels contribute to the observed increase of the measured TCS. Experiments and calculations for other targets suggest that the dominating contribution to this enhancement should be attributed to the elastic scattering (e.g. Boesten *et al* 1992, Tanaka *et al* 1999). Around 8.5 eV, the TCS energy function has a maximum of $40.8 \times 10^{-20} \text{ m}^2$ and then slightly decreases, being nearly constant within 10–20 eV ($40.2 \times 10^{-20} \text{ m}^2$). This broad feature may be attributed to numerous weak resonant structures which overlap in this energy range, but it may also arise due to nonresonant inelastic processes. From 20 eV, the TCS starts to decrease with increasing energy and close to 28 eV it has the minimum of $38 \times 10^{-20} \text{ m}^2$.

Above 30 eV, the cross section curve increases again and reaches the maximum of about $44 \times 10^{-20} \text{ m}^2$ around 50 eV. A comparison of TCSs for HFA and its hydrogen-substituted analogue, acetone (figure 3), indicates that the 50 eV energy TCS structure for e^- –HFA scattering reflects the presence of fluorine atoms in the HFA molecule. This observation is consistent with our earlier conclusions that the intermediate-energy broad TCS enhancement is a characteristic for perfluorinated molecules (e.g. Szmytkowski and Ptasinska-Denga 2001, Szmytkowski *et al* 2004). Beyond 50 eV the

TCS decreases steadily with increasing energy and at 400 eV the TCS falls to $17.6 \times 10^{-20} \text{ m}^2$. A change in the slope perceptible around 120 eV can be related to the ionization processes; the electron-impact ionization cross section for the HFA molecule has a maximum in this energy range (see table 2).

4.2. Comparison of electron-scattering cross sections for hexafluoroacetone and acetone: the perfluorination effect

Figure 3 compares the present electron-scattering TCS measured for HFA to that for the acetone ((CH₃)₂CO) molecule (Kimura *et al* 2000, Szmytkowski 2010). It is clearly evident that the perfluorination significantly changes the interaction of electrons with molecules over the entire energy range studied: the TCSs for HFA and acetone differ distinctly in the shape and magnitude. Fluorine atoms substituted for hydrogens not only change the size of the molecule but also influence essentially the electric charge distribution. While the acetone molecule possesses a high permanent electric dipole moment ($\mu_A = 2.88 \text{ D}$, Lide 1995–1996), the HFA molecule appears to be much less polar ($\mu_{\text{HFA}} \simeq 0.39\text{--}0.65 \text{ D}$; cf table 3).

Below 30 eV, the TCS for acetone is systematically higher than the TCS for HFA and the divergence distinctly increases towards lower energies. Due to the high electric dipole moment of the acetone molecule, the low-energy scattering for this target is dominated by direct processes; below 2 eV, the appearance of the TCS energy function for acetone reminds one rather of the Born integral cross section, $\sigma \sim \mu^2/E$ (Altshuler 1957), and considerably exceeds that for HFA.

Above 30 eV, the relation between compared TCSs reverses—the TCS for HFA becomes consistently higher. Such a relationship of intermediate-energy TCSs is a common feature of perfluorocarbons and their hydrocarbon homologues (e.g. Szmytkowski and Ptasińska-Denga 2001, Szmytkowski and Kwitniewski 2003), and may be, in general, related to the larger size of the perfluorinated target. Present calculations (cf table 2) show that the increase of the intermediate-energy TCS for HFA over that for acetone must be mainly related to the increase of the elastic-scattering contribution to the TCS for the fluorine-containing compound; for HFA, it amounts of 60–65%, nearly 10% more than for acetone. The increase in the ionization cross section for HFA and the shift of its maximum to higher energies are also noteworthy.

As can be seen in figure 3, above 70 eV the experimental TCSs for HFA and acetone are satisfactorily reproduced with the respective sums (ECS + ICS) of calculated ECS and ICS; for both molecules, differences between measured and calculated TCSs do not exceed the experimental uncertainties.

5. Conclusions

We have measured the absolute total electron-scattering cross section for the (CF₃)₂CO molecule in the linear electron-transmission experiment from low (1 eV) to intermediate (400 eV) energies. The experimental TCS shows two pronounced enhancements. The first one, visible between 2 and 28 eV, can in part be explained with resonant processes.

The second enhancement, with the maximum around 50 eV, is typical for fluorinated compounds. A comparison of the TCSs for HFA and acetone reveals a distinct perfluorination effect over the entire electron impact energy range investigated. At intermediate energies, the sum (ECS + ICS) of calculated elastic and ionization cross sections is in good agreement with the experimental TCS. This agreement enables us to suggest that the TCSs calculated this way may be useful for describing the TCS behaviour at intermediate and high energies for molecules for which experimental electron-scattering data are not accessible.

Acknowledgments

The authors gratefully acknowledge the support by the Polish Government (MNSzW) Research Funds for 2009–2010. The numerical computations have been performed at the CI TASK.

References

- Altshuler S 1957 *Phys. Rev.* **107** 114–7
- Bederson B and Kieffer L J 1971 *Rev. Mod. Phys.* **43** 601–40
- Bettega M H F and Lima M A P 2007 *J. Chem. Phys.* **126** 194317
- Boesten L, Tanaka H, Kobayashi A, Dillon M A and Kimura M 1992 *J. Phys. B: At. Mol. Opt. Phys.* **25** 1607–20
- Boudaïffa B, Cloutier P, Hunting D, Huels M A and Sanche L 2000 *Science* **287** 1658–60
- Cederbaum L S 1975 *J. Phys. B: At. Mol. Phys.* **8** 290–303
- Chan R K 1969 *Can. J. Chem.* **47** 2253–6
- Christophorou L G and Olthoff J K 2004 *Fundamental Electron Interactions with Plasma Processing Gases* (New York: Kluwer/Plenum) p 682
- Domaracka A, Możejko P, Ptasińska-Denga E and Szmytkowski Cz 2006 *J. Phys. B: At. Mol. Opt. Phys.* **39** 4289–99
- Domaracka A, Możejko P, Ptasińska-Denga E and Szmytkowski Cz 2007 *Phys. Rev. A* **76** 042701
- Frisch M J *et al* 2003 GAUSSIAN 03, Revision B.05 (Pittsburgh, PA: Gaussian)
- Grabow J-U, Heineking N and Stahl W 1991 *Z. Naturf. a* **46** 229–32
- Harland P and Thynne J C J 1969 *J. Phys. Chem.* **73** 2791–2
- Harland P and Thynne J C J 1970 *J. Phys. Chem.* **74** 52–9
- Hilderbrandt R L, Andreassen A L and Bauer S H 1970 *J. Phys. Chem.* **74** 1586–92
- Hwang W, Kim Y K and Rudd M E 1996 *J. Chem. Phys.* **104** 2956–66
- Itikawa Y 1978 *Phys. Rep.* **46** 117–64
- Khakoo M A, Muse J, Campbell C, Lopes M C A, Silva H, Winstead C and McKoy V 2009 *J. Phys.: Conf. Ser.* **194** 012027
- Kim Y K and Rudd M E 1994 *Phys. Rev. A* **50** 3954–67
- Kimura M, Sueoka O, Hamada A and Itikawa Y 2000 *Adv. Chem. Phys.* **111** 537–622
- Knudsen M 1910 *Ann. Phys., Lpz.* **31** 205–29
- Lide D R 1995–1996 *CRC Handbook of Chemistry and Physics* 76th edn (Boca Raton, FL: CRC)
- Maljković J B, Milosavljević A R, Blanco F, Šerić D, Garcia G and Marinković B P 2009 *Phys. Rev. A* **79** 052706
- Martin I 2007 *PhD Dissertation* Freien Universität, Berlin
- Martin I, Langer J, Stano M and Illenberger E 2009 *Int. J. Mass Spectrom.* **280** 107–12
- Mazurek U, Schröder D and Schwarz H 2002 *Angew. Chem. Int. Ed.* **41** 2538–41
- Miller K J 1990 *J. Am. Chem. Soc.* **112** 8533–42, 43–51
- Mott N F and Massey H S W 1965 *The Theory of Atomic Collisions* (Oxford: Oxford University Press)

- Możejko P, Żywicka-Możejko B and Szmytkowski Cz 2002 *Nucl. Instrum. Methods Phys. Res. B* **196** 245–52
- Możejko P and Sanche L 2003 *Radiat. Environ. Biophys.* **42** 201–11
- Możejko P and Sanche L 2005 *Radiat. Phys. Chem.* **73** 77–84
- Naff W T, Compton R N and Cooper C D 1972 *J. Chem. Phys.* **57** 1303–7
- Nelson R N and Colgate S O 1973 *Phys. Rev. A* **8** 3045–9
- von Niessen W, Schirmer J and Cederbaum L S 1984 *Comput. Phys. Rep.* **1** 57–125
- Ortiz J V 1988 *J. Chem. Phys.* **89** 6348–52
- Padial N T and Norcross D W 1984 *Phys. Rev. A* **29** 1742–8
- Pedrew J P and Zunger A 1981 *Phys. Rev. B* **23** 5048–79
- Raj D 1991 *Phys. Lett. A* **160** 571–4
- Salvat F, Martinez J D, Mayol R and Parellada J 1987 *Phys. Rev. A* **36** 467–74
- Sullivan J P, Makochekanwa C, Jones A, Caradonna P, Slaughter D S, Machacek J, McEachran R P, Mueller D W and Buckman S J 2011 *J. Phys. B: At. Mol. Opt. Phys.* **44** 035201
- Szmytkowski Cz 2010 *J. Phys. B: At. Mol. Opt. Phys.* **43** 055201
- Szmytkowski Cz, Domaracka A, Możejko P and Ptasińska-Denga E 2007 *Phys. Rev. A* **75** 052721
- Szmytkowski Cz and Kwitniewski S 2003 *J. Phys. B: At. Mol. Opt. Phys.* **36** 2129–38, 4865–73
- Szmytkowski Cz and Możejko P 2001 *Vacuum* **63** 549–54
- Szmytkowski Cz and Możejko P 2006 *Opt. Appl.* **36** 543–50
- Szmytkowski Cz, Możejko P and Kasperski G 1997 *J. Phys. B: At. Mol. Opt. Phys.* **30** 4363–72
- Szmytkowski Cz, Możejko P, Ptasińska-Denga E and Sabisz A 2010 *Phys. Rev. A* **82** 032701
- Szmytkowski Cz, Piotrowicz M, Domaracka A, Kłosowski Ł, Ptasińska-Denga E and Kasperski G 2004 *Phys. Rev. A* **74** 012708
- Szmytkowski Cz and Ptasińska-Denga E 2001 *Vacuum* **63** 545–8
- Tanaka H, Tashibana Y, Kitajima M, Sueoka O, Takaki H, Hamada A and Kimura M 1999 *Phys. Rev. A* **59** 2006–15
- Thynne J C J 1968 *Chem. Commun.* 1075–6
- Zakrzewski V G and von Niessen W 1994 *J. Comput. Chem.* **14** 13–8
- Zhang X, Sun J and Liu Y 1992 *J. Phys. B: At. Mol. Opt. Phys.* **25** 1893–7